Plasma Physics Reports, Vol. 29, No. 12, 2003, pp. 1034–1040. Translated from Fizika Plazmy, Vol. 29, No. 12, 2003, pp. 1114–1121.

PLASMA DYNAMICS

Experimental and Numerical Studies of Plasma Production in the Initial Stage of Implosion of a Cylindrical Wire Array

V. V. Aleksandrov*, A. G. Alekseev*, V. N. Amosov*, M. M. Basko, G. S. Volkov*, E. V. Grabovskiĭ*, A. V. Krasil'nikov*, G. M. Oleĭnik*, I. N. Rastyagaev*, P. V. Sasorov**, A. A. Samokhin*, V. P. Smirnov*, and I. N. Frolov***

**Troitsk Institute for Innovation and Fusion Research, Troitsk, Moscow oblast, 142190 Russia*

***Institute of Theoretical and Experimental Physics, Bol'shaya Cheremushkinskaya ul. 25, Moscow, 117259 Russia*

Received February 18, 2003; in final form, May 16, 2003

Abstract—The features are studied of plasma production in the initial stage of implosion of hollow cylindrical wire arrays at electric-field growth rates of 10^{12} V/(cm s). The results are presented from the analysis of both UV emission from the wire plasma and the discharge parameters in the initial stage of the formation of a Z-pinch discharge. It is found that, a few nanoseconds after applying voltage to a tungsten wire array, a plasma shell arises on the wire surface and the array becomes a heterogeneous system consisting of metal wire cores and a plasma surrounding each wire (a plasma corona). As a result, the current switches from the wires to the plasma. A further heating and ionization of the wire material are due primarily to heat transfer from the plasma corona. A model describing the primary breakdown along the wires is created with allowance for the presence of low-*Z* impurities on the wire surface. © *2003 MAIK "Nauka/Interperiodica".*

1. INTRODUCTION

Implosion of cylindrical arrays (liners) made of micron tungsten or aluminum wires under the action of nanosecond current pulses has been studied since the late 1980s [1–4]. Due to the implosion of the wire array material, a Z-pinch discharge is formed near the array axis. In the final stage of the Z-pinch implosion, an intense soft X-ray pulse is generated that can be used in inertial confinement fusion (ICF) research, in studying fundamental physical problems (such as the equation of state of a substance with extreme parameters), and in certain practical applications.

In [1], it was shown that the main factor governing the implosion dynamics of a cylindrical wire array is the prolonged (up to the current maximum) production of the wire plasma. Recent studies [5–7] showed that the plasma on the wire surface is produced in the first few nanoseconds after the current starts to flow through the wire array. After the plasma is produced, the current switches from the wires to the plasma corona. In this case, the wire array becomes a heterogeneous system consisting of a cylindrical metal wire core and a plasma corona surrounding the wires. A further heating and ionization of the wire material is primarily due to heat transfer from the plasma corona. Plasma production from a single wire by microsecond current pulses was described in [8]. In the nanosecond range, plasma production was studied in detail in [9].

Important factors characterizing the initial state of the plasma-producing medium are the nonuniformity of the distribution of the plasma sources and the nonuniformity of the plasma production rate along the wires. The nonuniformity of the distribution of the plasma sources can lead to the onset of various instabilities during plasma implosion, whereas the nonuniformity of the plasma production rate can result in a nonsimultaneous radial implosion of the plasma in different points along the array axis. Both these factors impede synchronous and compact implosion and, accordingly, decrease the emission power.

In this paper, we present the results of studying the initial stage of plasma production on the surfaces of tungsten wires during the implosion of a cylindrical wire array. By the initial stage of the formation of a Z-pinch discharge from a wire array, we mean the first 10–15 ns from the beginning of the current pulse, when the discharge current through a single wire is lower than 5 kA.

2. ARRANGEMENT OF THE EXPERIMENT

As wire liners, we used cylindrical hollow arrays assembled of eight or sixteen tungsten wires that were equally spaced along a cylindrical surface 8 or 20 mm in diameter. The array length was 10 mm. The diameter of the tungsten wires varied from 4 to 10 μm.

The scheme of connection of the wire array to the voltage source is shown in Fig. 1. The wire array was placed in the vacuum chamber of the ANGARA-5-1 facility [10]. The chamber was evacuated by oil-diffusion pumps. As a voltage source, we used one of the modules of the ANGARA-5-1. Because of this, the results obtained with arrays made of eight or sixteen wires in a single module could be compared with the

1063-780X/03/2912-1034$24.00 © 2003 MAIK "Nauka/Interperiodica"

implosion of arrays assembled of much greater number of wires (64 or 128) in the full-scale experiments carried out in the ANGARA-5-1.

The microsecond prepulse of the voltage generator was suppressed by using a prepulse spark gap placed in front of the wire liner. The prepulse was suppressed to such extent that the electric field strength at the array was lower than 10 V/cm and the increase in the wire temperature during the prepulse was lower than 10°C.

To study the initial stage of plasma generation, the discharge current through the array was measured simultaneously with the voltage drop across the array. The current through the array was measured by a shunt with a time resolution of 5 ns.

A resistive divider for measuring the voltage on the axis of the wire array was connected coaxially to the anode and, with the help of a metal rod aligned with the array axis, to a cathode. The time resolution of the divider was 2 ns.

Since, in these experiments, we were dealing with rapidly varying currents, the voltage measured by the divider differed from the voltage across the wire by an inductive term proportional to the rate at which the magnetic flux in the circuit formed by the wire surface and divider connectors varied. In order to determine the voltage across the wire surface, this term should be subtracted from the divider readings. A specific feature of the voltage measurements on the array axis is that the contribution of the inductive term is very small and can be ignored. The reason for this is that the magnetic field produced by the current flowing through the array is mainly localized on the outside of the array and the interlinkage between the generator circuit and the divider circuit is weak.

Plasma generation on the wire surface was detected by the appearance of UV emission. As a UV detector, we used a diamond sensor made of natural Yakut diamond. The detector was devised and fabricated in the Troitsk Institute for Innovation and Fusion Research [11, 12].

The detector was placed at a distance of 3.6 m from the wire array. A 1-mm-thick quartz glass was placed in front of the detector. The relative spectral sensitivity of the detector with the quartz glass is shown in Fig. 2. The time resolution of the detector was 2 ns.

The time resolution of the optical frame system for recording the wire array images was 10 ns. The spatial resolution of the images was 40 μm, the depth resolution being about 2 mm. The dynamic range of the measurement system was about 20.

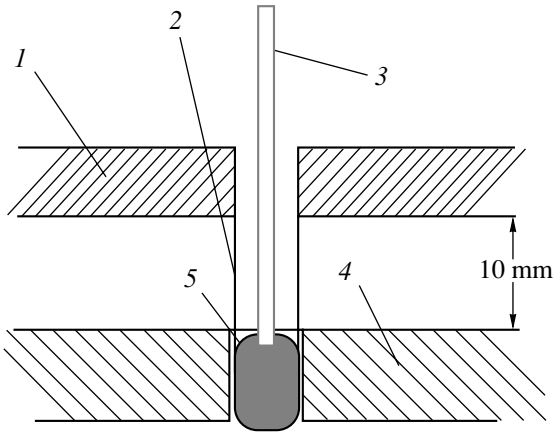

Fig. 1. Scheme of connection of the wire array and voltage divider to the voltage source: (*1*) anode of the ANGARA-5-1 facility, (*2*) wires, (*3*) metal rod connecting the voltage divider to the cathode, (*4*) cathode of the facility, and (*5*) cathode electrode of the wire array.

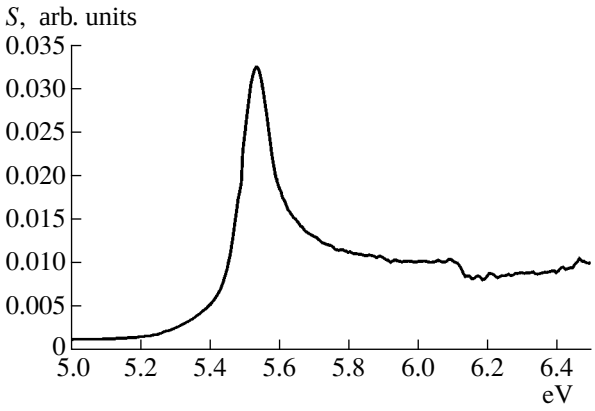

Fig. 2. Relative spectral sensitivity *S* of a diamond detector with a quartz glass.

3. EXPERIMENTAL RESULTS AND THEIR COMPARISON WITH NUMERICAL SIMULATIONS

3.1. Breakdown along the Wire Surface

The waveforms of the voltage on the axis of the system for several shots made with wire arrays and a single shot without wires (the no-load operating regime) are shown in Fig. 3. Without a wire array, the voltage on the axis during the first 50 ns was equal to the generator output voltage. During the first 20 ns, the maximum voltage drop across tungsten arrays with different outer diameters, different number of wires, and different wire diameters was in the range from 5 to 18 kV. The measured voltage pulses turned out to be substantially lower and shorter than the those measured in the no-load operating regime (without an array).

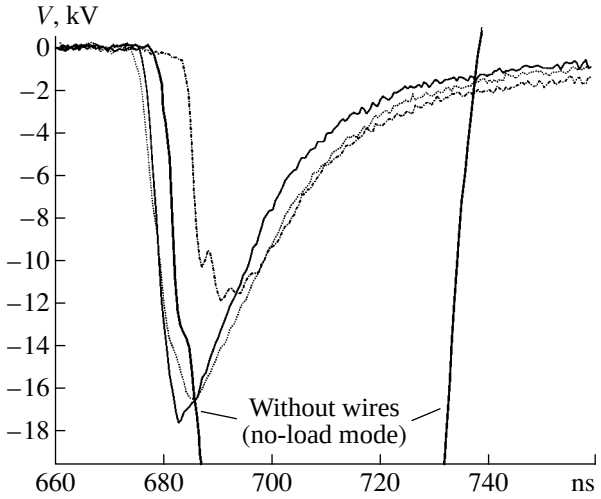

Fig. 3. Waveforms of the voltage on the axis for several shots with a wire array and a single shot without wires (the no-load operating mode).

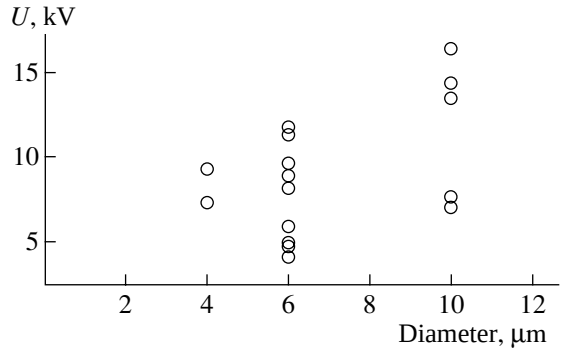

Fig. 4. Peak amplitude of the liner voltage U as a function of the tungsten wire diameter.

Estimates of the wire resistance at the instant corresponding to the maximum voltage showed that it was lower than the initial resistance of the cold wires. Note that the decrease in the resistance of the heated current-carrying metal wires can only be explained by the production of a low-resistive plasma on the wire surface.

Figure 4 shows the maximum voltage at the array as a function of the diameter of tungsten wires. It can be seen that the maximum voltage at the array somewhat increases with increasing wire diameter.

Figure 5 shows the waveforms of the voltage on the wire array axis and the intensity of UV emission. The presence of UV emission means that a plasma is produced on the wire surface. The delay time of the UV pulse with respect to the voltage pulse varies from 6 to 10 ns in different shots.

Figure 6a shows typical waveforms of the voltage on the liner axis, $U(t)$, and the current per one wire, $J(t)$, for a 8-mm-diameter wire array consisting of eight 10-μm tungsten wires. The results of processing of these signals are shown in Fig. 6b. These are three kinds of resistance per one wire: the total load resistance, $R_l(t)$; the wire resistance itself, $R_w(t)$; and the resistance of the plasma on the wire surface, $R_p(t)$. The total load resistance was calculated as the ratio $R_l(t) = U(t)/J(t)$. It can be seen that the ratio $U(t)/J(t)$ first increases due to the Joule heating of the wire and then decreases. The resistance $R_w(t)$ of a metal wire was calculated from the signal $U(t)$, taking into account the thermal resistivity coefficient, assuming that the entire electric power $U_2(t)/R_w(t)$ deposited in the wire is converted into heat, and ignoring energy losses by radiation and heat transfer. The plasma resistance $R_p(t)$ was calculated assuming that the plasma and metal wires are connected in-parallel and using the formula: $J(t)/U(t) = 1/R_w(t) + 1/R_p(t)$. A comparison of the time evolution of the plasma resistance with the recorded UV signal shows that the UV emission appears when the wire array resistance is already completely determined by the plasma resistance.

From the measurements of the load current and voltage in the initial stage of the process (before the plasma was produced on the wire surface), we could calculate the energy deposited in the wires due to ohmic heating. The calculations showed that, in most shots, the maximum temperature to which the tungsten wires were heated before the plasma was produced was lower than 2000°C. This temperature is substantially lower than the melting temperature of tungsten (3380°C).

The natural question arises as to why a plasma is produced on the wire surface.

The increase in the wire temperature during heating leads to the evaporation of low-Z impurities from the wire surface. As a result, a thin gas shell is formed near the surface. This shell is then broken, which results in plasma production. Additional experiments in which a current of ~3 A per wire was passed through the wire array for a time longer than 5 μs showed that a temperature of 300–400°C was sufficient to evaporate the layer of a low-Z coating material and produce plasma near the wire surface. Due to the rapid plasma expansion, the cross section of the current-carrying plasma channel increases, which leads to a sharp decrease in the channel resistance. The results of numerical simulations of the plasma production on the surface of a tungsten wire with a low-Z impurity coating is presented in the next section.

As was shown in [13], the breakdown of the produced gas shell can be initiated by electron emission from the wire surface. The emission is enhanced by the strong radial electric field that appears at some segment of a small-diameter wire at a certain configuration of electrodes. This field can exceed the axial electric field at the wire by a factor of 10 to100. The dependence of this effect on the wire diameter will be discussed at the end of the present paper.

Due to the presence of plasma on the wire surface, the current switches from the wires to the plasma. The main current begins to flow through the plasma, thereby heating it. A further heating of the wires is mainly due to heat transfer from the hot plasma to the wire surface. In this case, the contribution of the current flowing directly through the wires is relatively small.

We note that the warming of wires in vacuum to redness before an experiment had little effect on both the production of the surface plasma and the time evolution of the array resistance.

3.2. Numerical Simulations of Plasma Production on the Surface of a Tungsten Wire with and without Coating

To gain a better insight into the above experiments on measuring the time evolution of the resistance of a wire array under the action of a high-power current pulse, we carried out numerical simulations of this process. The simulations were performed using the NPINCH one-dimensional (radius–time) magnetohydrodynamic code [14, 15]. This code was improved by introducing an equation of state for metals over a wide range of densities and temperatures [16]. The equation of state takes into account the phase transition from a condensed to a gaseous state, and then to plasma, but ignores the transitions between the solid and liquid states. To calculate the kinetic coefficients of a condensed substance (the electron thermal conductivity, electric conductivity, heat exchange rate between ions and electrons, etc.), we used the procedure described in [17]. For the gas–plasma domain, we used the procedure described in [18]. The latter procedure is based on the well-known formulas for a hot magnetized plasma [19]. We simulated the time evolution of a 6-μm tungsten wire under the action of a given current pulse with a maximum amplitude of about 1 kA and a rise time of 20 ns.

The simulations were performed for both uncoated tungsten wires and wires coated by a thin layer of a low-Z material (carbon), which modeled a low-Z impurity on the tungsten surface. The calculation results are shown in Fig. 7.

The given time dependence of the current through an uncoated wire and the calculated waveform of the electric field strength on the wire axis are shown in Fig. 7a. It can be seen that, in this case, the electric field reaches 120 kV/cm, which is several times higher than the experimental value. This result confirms our assumption that, in real experiments, wires can never be considered clean. The decrease in the amplitude of the liner voltage can be explained by the presence of a thin low-Z coating on wires. Such a coating may be due to the deposition of vacuum oil vapor on a wire or the technology of wire fabrication.

To clarify the influence of the low-Z impurity coating on the electric characteristics of a wire, we divided

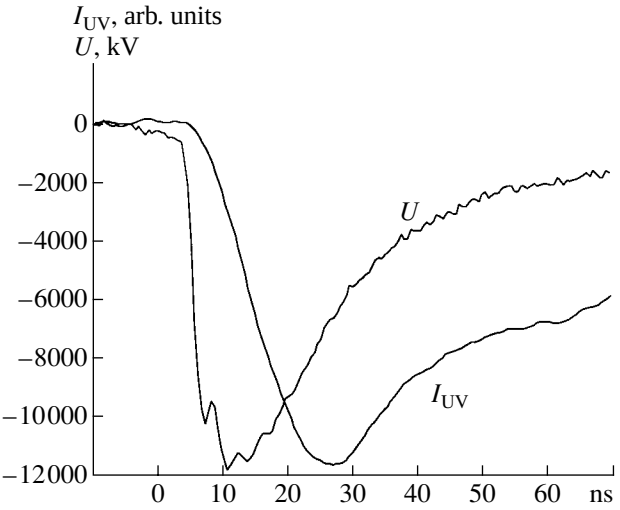

Fig. 5. Waveforms of the voltage on the array axis (U) and intensity of UV emission (I_{UV}) for an array consisting of eight 6-μm tungsten wires.

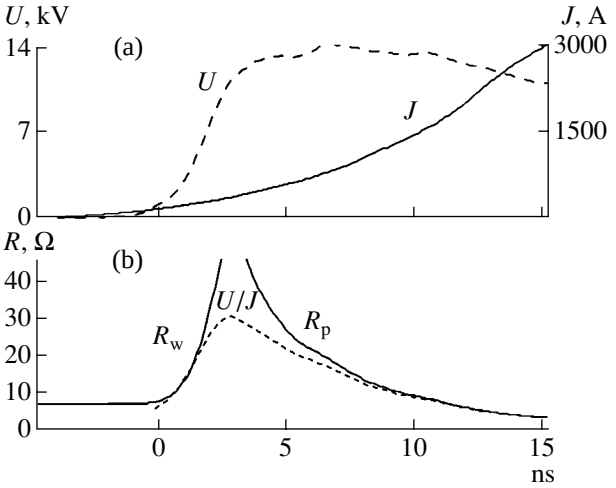

Fig. 6. (a) Waveforms of the voltage $U(t)$ across an 8-mm-diameter wire array consisting of eight 10-μm tungsten wires and the current through one wire $J(t)$. (b) Time evolution of the resistances (per one wire) calculated from the voltage and current waveforms: the total load resistance $U(t)/J(t)$, the wire resistance $R_w(t)$, and the resistance of the surface plasma $R_p(t)$.

a simulation into two stages. In the first stage (up to 6.75 ns), the heating of a clean wire was calculated. At the end of this stage, the temperature on the tungsten wire surface was 0.05 eV. The calculation was then continued assuming that the wire was coated with a 0.3-μm carbon layer in a gaseous state (with a mass per unit length of 1.8×10^{-10} g/cm). Thus, we simulated the primary evaporation of the low-Z coating. The calculated waveform of the voltage across a coated wire is shown in Fig. 7b. In this case, both the voltage amplitude and

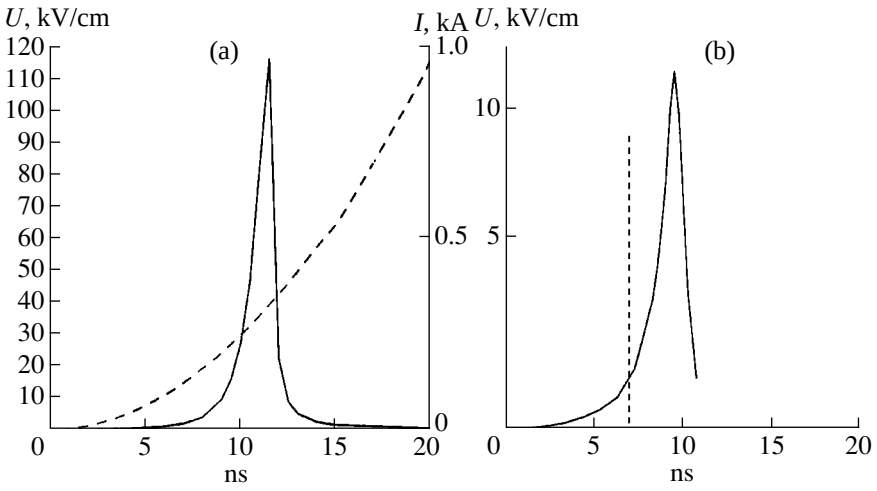

Fig. 7. Calculated waveforms of the electric field at the axis of a 6-μm tungsten wire during the current pulse: (a) an uncoated wire (the solid and dotted curves show the electric field and current, respectively, and (b) a wire coated with a model gaseous carbon shell with a density per unit length of 1.8×10^{-10} g/cm (the solid curve shows the electric field, and the vertical dotted line indicates the instant of evaporation of the coating).

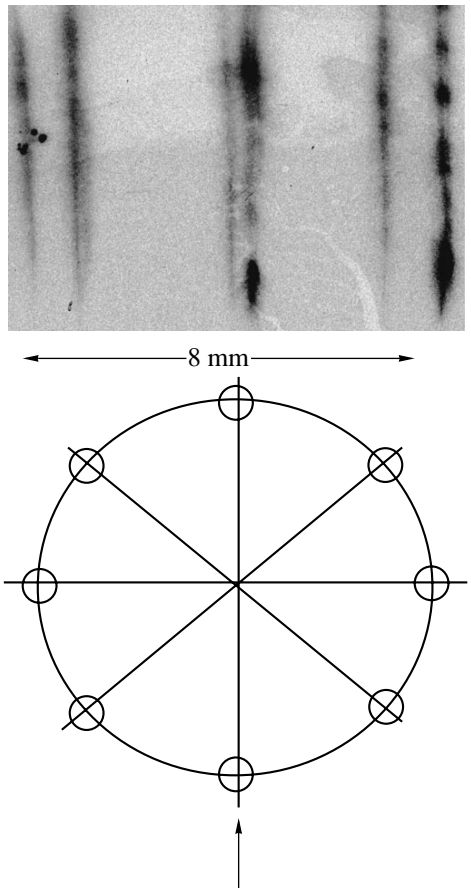

Fig. 8. Visible-light image of an array consisting of 7.5-μm eight tungsten wires with a current of 3 kA per wire. A schematic of the wire array and the viewing direction are shown at the bottom.

the shape of the voltage pulse are much closer to the experimental results. Breakdown along the wire is delayed from the beginning of the second stage by 2.5 ns, which is required for the necessary reduction in the density of the evaporated material due to expansion. Just after the breakdown of the gas shell and the formation of a plasma corona, the main current begins to flow through the corona, thereby heating it, and the Joule heating of the wire almost terminates. Up to this time, the characteristic tungsten temperature is 0.23 eV.

The above numerical simulations are only a rough approximation to the actual processes of the generation of a primary plasma and subsequent plasma production. Nevertheless, our model at least does not contradict the experimental data.

3.3. Spatial Nonuniformity of Plasma Generation

To study the process of energy deposition in a wire liner in the initial stage of implosion, we took frame-by-frame photographs of the liner in visible light. An image of an array consisting of eight 7.5-μm tungsten wires at the instant when the current reached a value of 3 kA per wire is given in Fig. 8. A characteristic feature of the liner image is a pronounced nonuniformity of the distribution of the emission intensity along the wire. The emission intensities of the individual wires are also slightly different. In the image, one can see well-defined regions with a nonuniform distribution of emission. The liner images testify to a nonuniform energy deposition in the wires in the initial stage of implosion. Note that the oscillations of the voltage on the array axis (see Fig. 5) may be attributed to the jitter in the breakdown time of the individual wires. This may be caused both by the factors affecting plasma production

(e.g., the nonuniformity of the impurity distribution along the wire) and by the onset of thermal and ionizational instabilities.

We note that the nonuniformity of the emission intensity along the wires begins to decrease when the current exceeds 5 kA per wire.

4. DISCUSSION OF THE RESULTS

4.1. Role of the Wire Diameter

Measurements of the electric characteristics of discharges through cylindrical hollow arrays made of tungsten wires showed that the wire-material plasma, which is generated near the wires several nanoseconds after the beginning of the current pulse, plays the dominant role in the development of the discharge. From this moment on, the wire array can be regarded as a heterogeneous system consisting of dense wire cores and a plasma corona surrounding the wires. Hence, the question arises as to mechanisms for plasma generation at such low values of the tangential electric field on the wire surface.

In [9], it was supposed that the radial electric fields can play an important role in initiating the breakdown of the gas evaporated from the wire surface. Because of the small wire diameter, the radial electric field can be higher than the axial field by a factor of 100 [13]. The smaller the wire diameter, the higher the radial electric field, all other factors being the same. This field is produced by the charges that are accumulated on the wires in the initial stage of the voltage pulse before breakdown (i.e., before the plasma is produced on the wire surface). After breakdown, these charges flow down onto the electrodes of the liner unit. The direction and strength of the radial electric field on the wire surface depend on the electrode configuration. When the wire is connected perpendicularly to two infinite plane-parallel electrodes that are at different potentials, the radial electric field is zero. For other electrode configurations, the radial field is nonzero. It may happen that, on one segment of the wire, the field is directed toward the wire, whereas on the other segment, it is directed away from the wire.

The field directed toward the wire can enhance electron emission from the wire surface and cause the electron-impact ionization of the gas shell surrounding the wire. In [13], it was shown that electron emission from the wire results in an electron current in crossed electric and magnetic fields outside the wire. Electrons from this flow can cause the heating and evaporation of not only impurities, but also of a thin ($\sim 10^{-3}$ μm) layer of the main wire material.

Gas breakdown occurs and plasma is produced at the instant when the gas density and electric field reach certain values. If surface gas breakdown on wires with different diameters takes place in the same radial field, then, for a thinner wire, gas breakdown will occur at lower values of the axial electric field because of the higher radial field on the wire surface. This conclusion is supported (in spite of the few statistics available and the large scatter in the data) by the results presented Fig. 4.

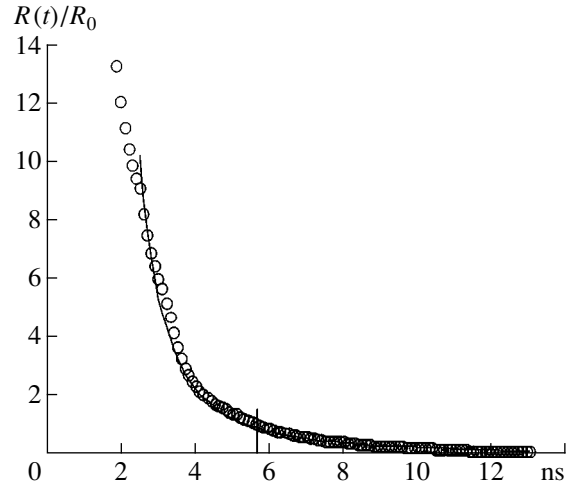

Fig. 9. Time evolution of the ratio of the plasma resistance near a single wire, $R(t)$, to the initial resistance of a cold wire, R_0. The circles show the experimental data, and the solid curve shows the result of simulations of an expanding plasma with an electron temperature of $T_e \sim 24$ eV. The instant at which the plasma resistance becomes equal to the resistance of the cold wire is indicated.

4.2. Estimates of the Plasma Parameters

Under some assumptions, we can estimate the parameters of the produced plasma from the observed time dependences of the liner voltage and current, as well as from the plasma resistance calculated using these dependences. Let us consider a rather rough model. Let the electron temperature of the plasma surrounding each wire be T_e [eV]. We assume that the plasma conductivity obeys the Spitzer law, the average ion charge number Z is proportional to $T_e^{0.5}$, and the velocity of plasma expansion into vacuum is determined by its temperature. It turns out that this model agrees best with the measured liner voltage and current for a tungsten plasma with an electron temperature of $T_e \sim 20$–30 eV. Figure 9 shows the waveforms of the ratio of the plasma resistance near a single wire to the initial resistance of a cold wire. One of the profiles is calculated from the measured voltage and current (circles), while the other profile is calculated using the above model for a tungsten plasma with an electron temperature of $T_e \sim 24$ eV (solid curve). The vertical line near 5.5 ns indicates the time when the plasma resistance becomes equal to the initial wire resistance. In this case, the velocity of plasma expansion into vacuum is $\sim 10^6$ cm/s. Hence, 10 ns after the plasma appears on the wire surface, the radius of the plasma column reaches ~100 μm. These simple estimates are

qualitatively consistent with the above numerical simulations of plasma production on the surface of a tungsten wire.

Unfortunately, such estimates cannot be extended to longer times because, at these times, the plasma radius becomes larger than the skin depth. In addition, the model ignores a very important factor, namely, the presence of a magnetic field. First, the magnetic field produced by the current flowing through the wire should impede plasma expansion. Second, the total magnetic field of all the wires should result in the acceleration of the current-carrying plasma toward the array axis under the action of the Ampére force.

The magnetic field produced by the wire array is lower than the magnetic field of a single wire by a factor $d/2\pi r$, where d is the distance between the wires and r is the wire radius. In view of the fact that the gas-kinetic plasma pressure on the wire surface exceeds the pressure of the magnetic field produced by the current flowing through a single wire, the Ampére force caused by the total current cannot substantially affect the expansion of the plasma column as a whole during the first 10 ns. This conclusion, however, results from the roughness of the model. The density of the tungsten ions on the boundary of the plasma column decreases smoothly. Inside the array, there is a region where the Ampére force can accelerate a small amount of a low-density plasma toward the array axis. This results in the appearance of a plasma precursor [1], whose velocity ($\sim 10^7$ cm/s) is one order of magnitude higher than the expansion velocity of the plasma column [13].

There are also other factors that are not taken into account by the above model, in particular, the nonuniform plasma production along the wires and the nonsimultaneous plasma production on different wires. That these factors really do exist can be seen in Fig. 8. However, even such a rough model has allowed us to estimate the plasma temperature and to obtain the lower estimate for the tungsten ion density from the measured current–voltage characteristics.

5. CONCLUSIONS

It has been found that, a few nanoseconds after the beginning of the current pulse, a plasma is produced on the wire surfaces and the wire array becomes a heterogeneous system consisting of the metal wires and the plasma on their surfaces. The current switches from the wires to the plasma. As a result, the resistance of the system decreases and, accordingly, the voltage drop across the array decreases. A further heating of the wires is primarily provided by the current flowing through the plasma and by heat transfer from the plasma, rather than by the current flowing through the wires.

ACKNOWLEDGMENTS

This work was supported in part by the Russian Foundation for Basic Research, project nos. 01-02-17319 and 01-01-17526.

REFERENCES

1. M. B. Bekhtev, V. D. Vikharev, S. V. Zakharov, *et al.*, Zh. Éksp. Teor. Fiz. **95**, 1653 (1989) [Sov. Phys. JETP **68**, 955 (1989)].
2. I. K. Aĭvazov, M. B. Bekhtev, V. V. Bulan, *et al.*, Fiz. Plazmy **16**, 645 (1990) [Sov. J. Plasma Phys. **16**, 373 (1990)].
3. R. B. Spielman, C. Deeney, G. A. Chandler, *et al.*, Phys. Plasmas **5**, 2105 (1998).
4. S. V. Lebedev, F. N. Beg, S. N. Bland, *et al.*, Phys. Plasmas **8**, 3734 (2001).
5. A. V. Branitskii, E. V. Grabovskii, M. V. Frolov, *et al.*, in *Proceedings of the 12th International Conference on High-Power Particle Beams, Haifa, 1998*, p. 599.
6. A. A. Aleksandrov, A. V. Branitskiĭ, G. S. Volkov, *et al.*, Fiz. Plazmy **27**, 99 (2001) [Plasma Phys. Rep. **27**, 89 (2001)].
7. A. Alexandrov, A. Branitskii, E. V. Grabovskii, *et al.*, in *Inertial Fusion Sciences and Application 99*, Ed. by Ch. Labaune, W. J. Hogan, and K. A. Tanaka (Elsevier, Paris, 1999), p. 621.
8. S. V. Lebedev and A. I. Savatinskiĭ, Usp. Fiz. Nauk **144**, 215 (1984) [Sov. Phys. Usp. **27**, 749 (1984)].
9. G. S. Sarkisov, B. S. Bauer, and D. S. De Groot, Pis'ma Zh. Éksp. Teor. Fiz. **73**, 74 (2001) [JETP Lett. **73**, 69 (2001)].
10. Z. A. Al'bikov, E. P. Velikhov, A. I. Veretennikov, *et al.*, At. Énerg. **68**, 26 (1990).
11. A. G. Alekseyev, V. N. Amosov, V. S. Khrunov, *et al.*, *Diagnostics for Experimental Thermonuclear Fusion Reactors*, Ed. by P. E. Stott, G. Gorini, and E. Sindoni (Plenum, New York, 1996).
12. S. F. Kozlov, US Patent No. 3668400 (June 6, 1972).
13. G. S. Sarkisov, P. V. Sasorov, K. W. Struve, *et al.*, Phys. Rev. E **66**, 046413 (2002).
14. N. A. Bobrova, T. L. Razinkova, and P. V. Sasorov, Fiz. Plazmy **18**, 517 (1992) [Sov. J. Plasma Phys. **18**, 269 (1992)].
15. N. A. Bobrova, S. V. Bulanov, T. L. Razinkova, and P. V. Sasorov, Fiz. Plazmy **22**, 387 (1996) [Plasma Phys. Rep. **22**, 349 (1996)].
16. M. M. Basko, Teplofiz. Vys. Temp. **23**, 483 (1985).
17. M. Basko, Th. Löwer, V. N. Kondrashov, *et al.*, Phys. Rev. E **56**, 1019 (1997).
18. N. A. Bobrova and P. V. Sasorov, Fiz. Plazmy **19**, 789 (1993) [Plasma Phys. Rep. **19**, 409 (1993)].
19. S. I. Braginskii, in *Reviews of Plasma Physics*, Ed. by M. A. Leontovich (Gosatomizdat, Moscow, 1963; Consultants Bureau, New York, 1965), Vol. 1.

Translated by E.L. Satunina